New Designed Procedure for G/SiO$_2$/SiC nano-heterojunctions Growth on Recycled 3C-SiC Powder

Maria Sarno[a], Sergio Galvagno[b], Rosangela Piscitelli[a], Sabrina Portofino[b], Claudia Cirillo*[a], Paolo Ciambelli[a]

a Department of Industrial Engineering DIIN and Research Centre NANO_MATES, University of Salerno, Via Giovanni Paolo II, 132, 84084 Fisciano (SA), Italy
b Department of Environment, Global Change and Sustainable Development, C.R. ENEA Portici, via Vecchio Macello loc. Granatello, 80055 Portici, Na, Italy
clcirillo@unisa.it

Few layer graphene/SiO$_2$/SiC (G/SiO$_2$/SiC) core-layers-sheath nano-heterojunctions were obtained by a new easy and cheap designed procedure by thermal annealing at atmospheric pressure and low temperature on 3C-SiC powder derived from exhausted activated carbon. Recycled SiC was chosen as growth substrate to realize a convenient process and to increase the added value of the recycled, combining the favourable properties of different substances. SiC powder and the advanced materials obtained were carefully characterized by the combining use of different techniques: transmission electron microscopy (TEM) with EDAX probe, scanning electron microscopy (SEM), X-ray diffraction analysis, Raman spectroscopy, thermogravimetric analysis coupled with quadrupole mass detector (TG-DTG-MASS).

1. Introduction

Graphene has attracted vast interest, in recent years, thanks to the very high number of application's fields. Silicon carbide is a wide-bandgap semiconductor with many interesting properties, such as high hardness, large thermal conductivity, a low coefficient of thermal expansion, and excellent resistance to erosion and corrosion. During the fast development of nanotechnology in the past decade, research effort has been focused on the preparation, thought different approaches, of nanometer-sized functional electronic devices. Nano-scaled electronic devices with a variety of functions may be realized by combining different nanomaterials. For the intrinsic characteristic of SiC and graphitic carbon, and looking at the possibility to obtain a metallic-insulator-semiconductor geometry, coaxial nanocable of SiC-SiO$_2$–carbon (Zhang et al., 1998; Li et al., 2004) and chains of carbon nanotubes-SiC, have been also prepared by CVD or reactive laser ablation (Panda et al., 2010; Cai et al., 2007). Although the thermal oxidation of SiC to SiO$_2$ is a common and know procedure in the microelectronic industry, it is rather complicated because the product could results in mixed oxides containing C species. Numerous paper have been published on this theme (Schürmann et al., 2006), one of the key aspect was the diffusion of CO and CO$_2$ molecules in SiO$_2$ during SiC oxidation, whereas a challenging goal was to avoid carbon intermixing in the SiO$_2$ interlayer and covering the outer surface by a carbon layer, e.g. few layer graphene. Here we report, for the first time, the preparation of few layer graphene/SiO$_2$/SiC (G/SiO$_2$/SiC) nanofilaments by a new designed procedures, consisting in a thermal annealing under few percents of oxygen in nitrogen of 3C-SiC powder, derived from exhausted activated carbon (Sarno et al., 2016), at atmospheric pressure and low temperature for their intrinsic advantages. The composite materials obtained were carefully characterized by the combining use of different techniques: transmission electron microscopy (TEM) coupled with an EDAX probe, scanning electron microscopy (SEM), Raman spectroscopy, thermogravimetric analysis (TG-DTG) coupled with a quadrupole mass detector and X-ray diffraction analysis.

2. Experimental

For G/SiO$_2$/SiC synthesis, SiC substrate was, first of all, annealed for 10 min under argon at 1200°C in order to uniform the surface removing residual polishing damage. Then, oxygen, 50 ppm in 100 cc(stp)/min of nitrogen, was fed to the reactor (Sarno et al., 2012) from room temperature to 1150°C and kept 1 hour at this constant temperature, followed by 15 min under pure hydrogen. Finally, the sample was treated for 30 min in argon to allow residual CO to diffuse out (Cooper, 1997).

All the obtained samples were characterized by the combined use of different techniques. Transmission electron microscopy (TEM) images were acquired using a FEI Tecnai electron microscope operated at 200 KV with a LaB$_6$ filament as the source of electrons, equipped with an EDX probe. Scanning electron microscopy (SEM) images were obtained with a LEO 1525 microscope. Raman spectra were obtained at room temperature with a micro-Raman spectrometer Renishaw inVia with a 514 nm excitation wavelength (laser power 30 mW) in the range 100-3000 cm^{-1}. Optical images were collected with a Leica DMLM optical microscope connected on-line with the Raman instrument. For all the samples about 40 measurements have been carried out. The laser spot diameter was about 10 µm. XRD measurements were performed with a Bruker D8 X-ray diffractometer using CuKα radiation. Thermogravimetric analysis (TG-DTG) at a 10 K/min heating rate in flowing air was performed with a SDTQ 500 Analyzer (TA Instruments).

3. Results and discussion

A typical TEM image of the synthesized sample is reported in Figure 1a, showing around the nanofilaments a layer of different colour of about 20 nm. An enlarged image of the nanofilaments is shown in Figure 1b, it displays a characteristic dark core and lighted sheath, with the nanofilament sheath about 20-30 nm thick. Chemical composition microanalysis, evidences the outer C sheath and the increased oxygen amount in the intermediate layer with respect to the core. Typical EDS spectra taken from three different zones (indicated as A, B, C in the inserts of Figure 1b) of a nanofilaments are depicted in Figure 1 A,B,C. The EDS results were confirmed by the high resolution TEM image observations (inserts in the Figure). They showed that the nanofilaments are indeed composed of a 3C-SiC core, a SiO$_2$ intermediate layer, and an outer layer of graphitic carbon. Twisted graphene layers (about 13 are counted in the insert of Figure 1b) with the typical (002) stacking of graphitic carbon are clearly visible for the outermost nanofilament layers.
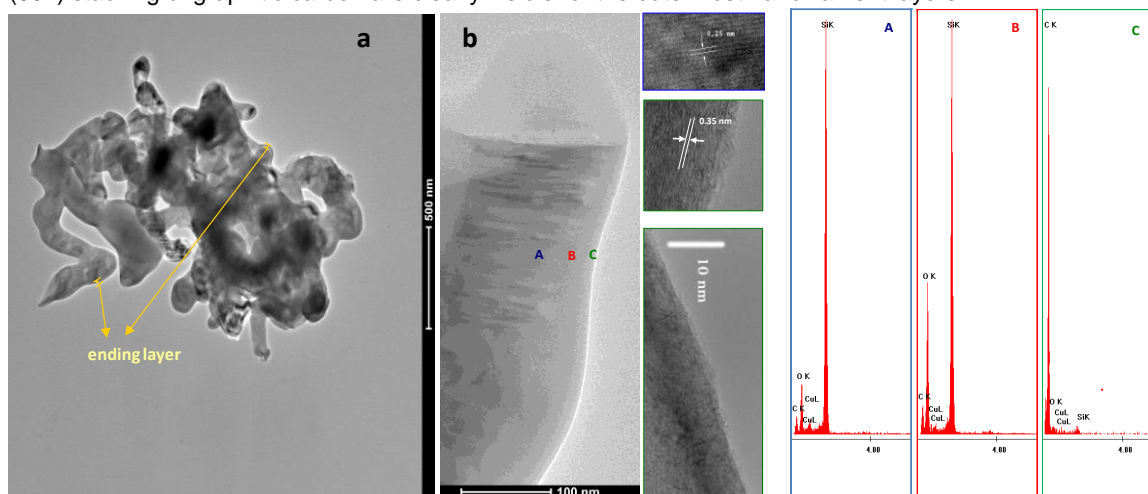

Figure 1: TEM image of G/SiO$_2$/SiC (a). Representative TEM images of the prepared nanofilaments of G/SiO$_2$/SiC composite. High resolution TEM images of coaxial nanofilaments, displaying single crystalline 3C-SiC core, SiO$_2$ intermediate layer and outer graphitic carbon sheaths. Energy dispersion spectra taken from different zones of the nanofilaments as marked in Figure 1b with A, B and C.

The Raman Spectrum reported in Figure 2a, collected on the G/SiO$_2$/SiC, clearly shows the multiphase nature of the sample, the band between 400 cm^{-1} and 500 cm^{-1} is due to SiO$_2$, on the other hand at higher cm^{-1} the spectrum results from the superimposition of SiC and sp^2 carbon. In particular, in the range 1200-3200 cm^{-1}, three additional bands appear at about 1346, 1588 and 2700 cm^{-1}, which are attributed respectively to the D, G and 2D carbon bands (Ouerghi et al., 2010). The presence of a single G and 2D bands indicates the thin thickness of the carbon layer (Ouerghi et al., 2010). The appearance of the D band indicates structural defect of edge in the few layers graphene formed. All the transverse optical (TO) and longitudinal optical (LO) are shifted towards low wavenumber region if compared with pristine 3C-SiC, the red shift of the Raman bands

might be due to the confinement effect, stacking faults and stress form the heterostructure of core shell G/SiO₂/SiC structure (Panda et al., 2010). The band at ~2960 cm⁻¹ is attributed to a superimposition of a pair of the combination bands: the D+G and D+D' bands, (D' is the shoulder in the G band typically present at ~1620 cm⁻¹) (Handa et al., 2011).

In addition to the typical peaks of SiC in the XRD spectrum of the G/SiO₂/SiC (Figure 2b) the strong peak at 21,9° due to SiO2 is also visible. The spectrum in the range 20-30° is characterized by a more noise than that of pristine 3C-SiC, on the other hand the (002) peak due to carbon stacking is no visible, suggesting a thin structure of few graphene and disorder for the carbon layers.
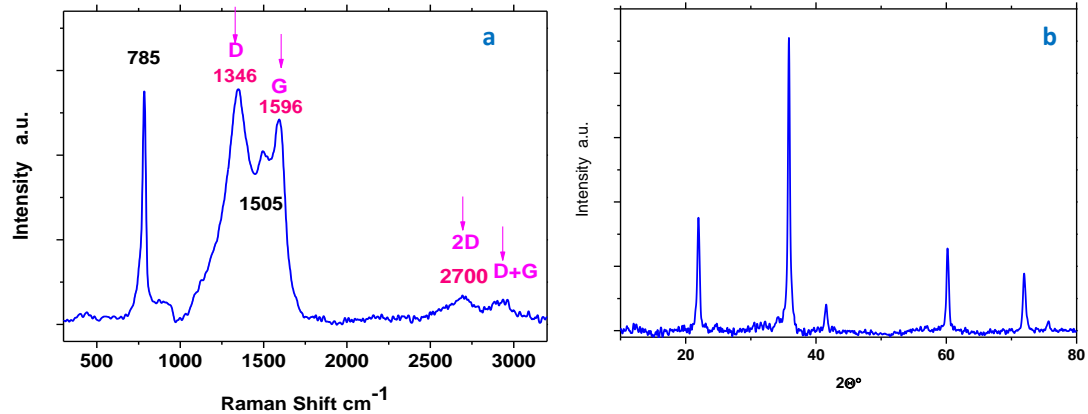

Figure 2: Raman spectrum of G/SiO₂/SiC (a) and X-ray diffraction spectrum of G/SiO₂/SiC (b).

Silicon carbide is a promising semiconductor to be used in metal-oxide-semiconductor devices, for this applications it is most advantageous that the oxidation of SiC leads to SiO2 passivated surface, as for the most popular Si technology. Therefore, numerous studies (Costello and Tressler, 1986; Mieskowski et al., 1984; Pultz, 1967) have been conducted on the oxidation of 4H- and 6H-SiC samples, and several models reported to explain it. Compared to thermal oxidation of Si, oxidation of SiC is more complicated. The oxidation process of silicon carbide is governed by the transport of molecular oxygen to the reaction front, the reaction of oxygen with SiC at the interface and the out diffusion of gases through the growing silicon oxide film.
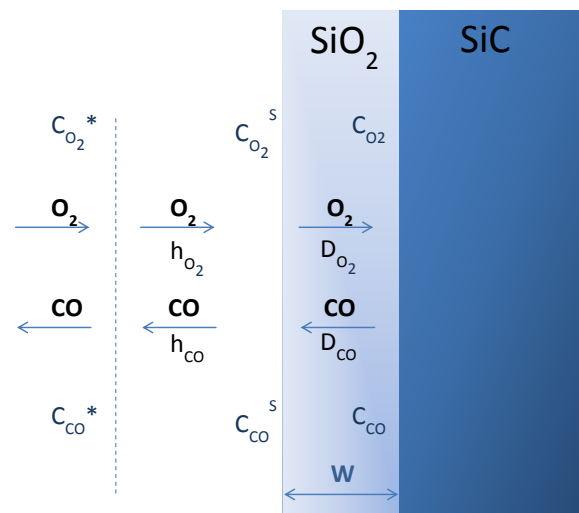
Scheme 1: The five steps during SiC oxidation.

There are five steps (see the Scheme 1) in the thermal oxidation of SiC: (i) diffusion of oxygen gas to the oxide surface; (ii) in-diffusion of oxygen through the oxide film (favoured the higher the oxygen partial pressure); (iii) reaction, at the oxide/SiC interface, with SiC (favoured by temperature, at given operating conditions, more than the others steps); (iv) out-diffusion of the produced gases through the oxide; (v) diffusion of the product gases away from the oxide surface.

In particular, looking to Scheme 1, the oxygen flux to the vicinity and in the SiO$_2$ bulk (Song et al., 2004) can be written as:

$$F_{O_2} = h_{O_2}(C_{O_2}^* - C_{O_2}^S)$$

$$F_{O_2} = D_{O_2}\frac{(C_{O_2}^S - C_{O_2})}{W}$$

where h_{O2} is the gas phase transport coefficient, D_{O2} the oxygen diffusivity in the metal bulk, and those for CO:

$$F_{CO} = h_{CO}(C_{CO}^S - C_{CO}^*)$$

$$F_{CO} = D_{CO}\frac{(C_{CO} - C_{CO}^S)}{W}$$

finally the flux corresponding to the oxidation rate are:

$$F = K_f C_{O,} - K_r C_{co}$$

where K_f and K_r are the rate constant of the forward and reverse reactions, respectively.

The first and last steps in general are not rate-controlling steps. Among the different other steps the rate limiting step is still uncertain as discussed in several articles (Jacobson, 1993; Luthra, 1991).

Depending on the oxidation conditions, various limiting processes are possible, influencing the characteristics of the oxidation process also giving rise to different reaction. In particular, four different reactions (Song and Smith, 2002) are predicted to be dominant, depending on P(O$_2$) and T, producing four different results (the experiments have been performed in the temperature range 1150-1600°C in pure oxygen P=0,001-100Pa).

- At low partial pressure of oxygen and high temperature the reaction:
  (2+x)SiC(s)+ O$_2$(g) → (2+x)Si(g)+2CO(g)+xC(s)   (1)
  is dominant, corresponding to an etching along with the formation of a carbon layer.
- The reaction:
  2SiC(s)+ O$_2$(g) → 2Si(g)+2CO(g)   (2)
  is predominant in the boundary conditions, between those of reaction (1) and (3). This reaction corresponds to the simultaneous vaporization and etching of SiC.
- At increasing partial pressure of oxygen and lower temperature, the reaction:
  2SiC(s)+ O$_2$(g) → SiO(g)+CO(g)   (3)
  happens, leading to an active oxidation or etching of the SiC.
- At still higher P(O$_2$) and lower temperature, the dominant reaction is
  2SiC(s)+ 3O$_2$(g) → 2SiO$_2$(s)+2CO(g)   (4)
  which product is commonly the desired product, i.e. the passivation of the SiC surface.

Although, at even higher partial pressure of O$_2$ than that used in the case of reaction (4), it has been predicted (Song and Smith, 2002); Jacobson, 1993; Luthra, 1991) that solid SiO$_2$ and C can be the only products.

Reaction (4) is the fundamental in the passivation of SiC. Most of the paper published, regarding the SiC oxidation, deal specifically on this reaction, in particular because during the SiC oxidation carbon contaminations can be easily observed either at the interface or incorporated in the silicon dioxide layer (Afanasev et al., 1997; Vathulya et al., 1998). Carbon atoms from the silicon carbide substrate leave the sample during the oxidation process. This happens via out-diffusion of CO molecules through the growing oxide film. These CO molecules determines the formation of carbon clusters or graphitic regions (Wang et al., 2001; Afanasev et al., 1996). Basically, a CO molecules, generated at the advancing interface and diffusing through the oxide can bind weakly to a O site in the SiO$_2$ network. A second CO molecules, however, can bind to the first forming a new very stable complex. Additional CO molecules can extend the cluster. The process is helped by a passing CO that takes an O atom from the cluster and effuses as CO$_2$. The net result is O-deficient cluster of carbon. To form a carbon layer on the outer surface and to have a controlled SO$_2$ thickness, we chose our operating conditions on the base of the literature overview, experimental evidences and the following considerations: (i) the partial pressure of oxygen has been chosen in order to be high enough to ensure that the oxygen diffusion is not the limiting step, otherwise the oxidation process can be influenced, also giving rise to different reaction than (4), with the formation of carbon (e.g. reaction (1)); (ii) temperature low enough to have a sort of chemical reaction/out diffusion controlling regime (a reaction too favored could lead to an oxygen diffusion controlling, in the growing SiO$_2$ film and/or a too fast CO out diffusion); (iii) a suitable reaction time to have a controlled SO$_2$ thickness (an O$_2$ diffusive regime can be also determined by increasing time and thus thickness of the silica layer, a complete CO out-diffusion can be

determined by a too low silica thickness). To promote a further carbon graphitization 15 min under pure hydrogen were performed, than 30 min in argon allows the residual CO to diffuse out (Cooper; 1997).

For the SiC oxidation, it has been reported, that the thermal growth kinetics is governed by linear parabolic law of Deal and Grove, as derived for Silicon (Afanasev et al., 1996; Schmeiber et al., 2001; Htun Aung et al., 2002).

$$W + AW = B(t + \tau)$$ (5)

Where, W denotes the oxide thickness and t is oxidation time. The quantity τ corresponds to a shift in the time coordinate that correct for the presence of the initial layer of oxide thickness and A and B are constants (B parabolic and B/A linear rate constant). The above equation is a quadratic equation.

The solution of equation (5) can be written as:

$$\frac{W}{A/2} = (1 + \frac{t + \tau}{A^2/4B})^{1/2} - 1$$

where A and B can be expressed as:

$$A = \frac{1 + \dfrac{1,5K_f}{h_{O_2}} + \dfrac{K_r}{h_{CO}}}{\dfrac{1,5K_f}{D_{O_2}} + \dfrac{K_r}{D_{CO_2}}} \qquad\qquad B = \frac{1 + \dfrac{1,5K_f}{h_{O_2}} + \dfrac{K_r}{h_{CO}}}{\dfrac{1,5K_f}{D_{O_2}} + \dfrac{K_r}{D_{CO_2}}}$$

According with references (Afanasev et al., 1996), the oxidation kinetic results linear when the interface reaction is the rate-controlling step:

$$\frac{B}{A} \approx \frac{C^*_{O_2}}{N_0} K_f$$

The kinetic is parabolic, if O_2 diffusion or CO out-diffusion are controlling:

$$B \approx \frac{C^*_{O_2}}{1.5 N_0} D_{O_2} \qquad\qquad B \approx \frac{C^*_{O_2} K_f}{N_0 K_r} D_{CO}$$

We evaluate the average oxide thickness as a function of time, see Figure 3, in the same operating conditions reported in the experimental section but temperatures (the tests were performed at 1150, 1200 and 1250°C), finding an activation energy of 2.74 eV, suggesting a CO-out diffusion/interface reaction limiting steps (Song et al., 2004).
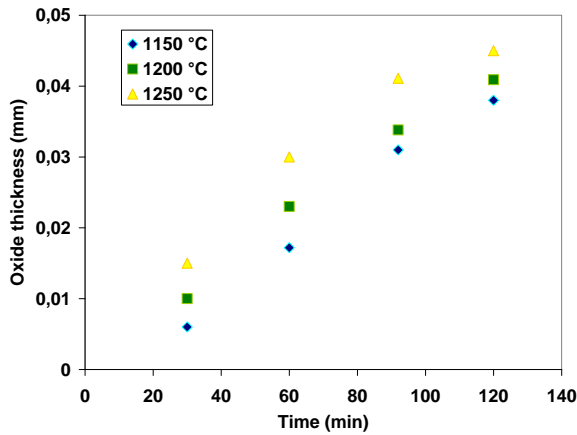

Figure 3: Oxide thickness as a function of time and temperature during tests performed in the same operating condition of the C/SiO₂/SiC synthesis but temperature.

4. Conclusion

Nanofilaments heterojunctions of few layer graphene/SiO_2/SiC core shell structure with a sheath of about 20-30 nm thick have been prepared by a new easy designed procedure. Chemical composition microanalysis, evidences the outer carbon sheath and the increased oxygen amount in the intermediate layer with respect to the core. The nanofilaments are composed of a 3C-SiC core, a SiO_2 intermediate layer, and an outer layer of graphitic carbon. Twisted graphene layers (about 13 are counted) with the typical (002) stacking of graphitic carbon are clearly visible in the outermost nanofilament layers.

Reference

Afanasev V.V., Bassler M., Pensl G., Schulz M. 1997, Intrinsic SiC/SiO_2 interface states, Phys. Status. Solidi. A. 162, 321-337.

Afanasev V.V., Stesmans A., Bassler M., Pensl G., Schulz M.J., Harris C.I. 1996, Elimination of SiC SiO_2 interface states by preoxidation ultraviolet-ozone cleaning, Appl. Phys. Lett. 68, 2141-2143.

Aung M.T.H., Szmidt J., Bakowski M. 2002, The study of thermal oxidation on SiC surface, J. Wide Bandgap Mater. 9, 313-318.

Cai, K.F., Zhang A.X., Yin, J.L. 2007, Ultra thin and ultra long SiC/SiO_2 nanocables from catalytic pyrolysis of poly(dimethylsiloxane), Nanotechnol. 18, 509901.

Cooper J.A. 1997, Advances in SiC MOS Technology. Phys. Stat. Sol. (a), 162, 305-320.

Costello J.A., Tressler R.E. 1986, Oxidation Kinetics of Silicon Carbide Crystals and Ceramics: I, In Dry Oxygen, J. Am. Ceram. Soc. 69, 674-681.

Jacobson N.S. 1993, Corrosion of silicon-based ceramics in combustion. J. Am. Ceram Soc. 76, 3-28.

Li Y., Bando Y., Golberg D. 2004, SiC–SiO_2–C Coaxial Nanocables and Chains of Carbon Nanotube–SiC Heterojunctions, Adv.Mater. 16, 93-96.

Luthra K.L. 1991, Some new perspectives on oxidation of silicon carbide and silicon nitride. J. Am. Ceram. Soc. 74, 1095-1103.

Mieskowski D.M., Mitchell T.E., Heuer A.H. 1984, Bubble formation in oxide scales on SiC. J. Am. Ceram. Soc. 67, C17-C18.

Panda S.K., Sengupta J., Jacob C. 2010, Synthesis of Beta-SiC/SiO_2 Core-Sheath nanowires by CVD technique using Ni as Catalyst, J. Nanosci. Nanotech. 10, 3046-3052.

Pultz W.W. 1967, Temperature and Oxygen Pressure Dependence of Silicon Carbide Oxidation, J. Phys. Chem. 71, 4556-4558.

Sarno M., Galvagno S., Piscitelli R., Portofino S., Ciambelli P. 2016, Supercapacitor Electrodes Made of Exausted Carbon-derived SiC Nanoparticles Coeted by Graphene, Ind. Eng. Chem. Res. 55, 6025-6035.

Sarno M., Sannino D., Leone C., Ciambelli P. 2012, Evaluating the effects of operating conditions on the quantity, quality and catalyzed growth mechanisms of CNTs, J. Mol. Catal. A-Chem. 357, 26-38.

Schmeiber D., Batchelor D.R., Mikol, R.P., Halfmann O., Spez A.L. 2001, Oxide growth on SiC (0001) surfaces, Appl. Surf. Sci. 184, 340-345.

Schürmann M., Dreiner S., Berges U., Westphal C. 2006, Investigation of carbon contaminations in SiO_2 films on 4H-SiC(0001), J. Appl. Phys. 100, 113510.

Song Y., Dhar S., Feldma, L.C., Chung G., Williams. J.R. 2004, Modified deal and grove model for the thermal oxidation of silicon carbide, J. Appl. Phys. 95, 4953-4957.

Song Y., Smith F.M. 2002, Phase diagram of the interaction of oxygen with SiC, Appl. Phys. Lett. 81, 3061-3063.

Vathulya V.R., Wang D.N., White M.H. 1998, On the correlation between the carbon content and the electrical quality of thermally grown oxides on p-type 6H–Silicon carbide, Appl. Phys. Lett. 73, 2161-2163.

Wang S., Di Ventra M., Kim S.G., Pantelides S.T. 2001, Atomic-scale dynamics of the formation and dissolution of carbon clusters in SiO_2, Phys. Rev. Lett. 86, 5946-5949.

Zhang Y., Suenaga K., Colliex C., Iijima S. 1998, Coaxial Nanocable: Silicon Carbide and Silicon Oxide Sheathed with Boron Nitride and Carbon, Science 281, 973-975.